

## EXPERIMENTAL REVIEW OF NEUTRINO PHYSICS

SHIGEKI AOKI

*for CHORUS and DONUT collaboration,  
Tsurukabuto, Nada, Kobe, 657-8501, JAPAN  
E-mail: aoki@kobe-u.ac.jp*

Dedicated to Prof. Masami Nakagawa who passed away in March 2001.

### 1 Introduction

#### 1.1 $\nu_e$

The first “detection” of the neutrino was the observation of a continuous spectrum of  $\beta$ -ray measured by Chadwick<sup>1</sup> in 1914. Here, “detection” means a discovery of experimental “indirect” evidence.

In 1956 (42 years later!), Cowan and Reines<sup>2</sup> observed interactions of anti-electron-neutrinos from a nuclear power reactor by the reaction  $\bar{\nu}_e + p \rightarrow n + e^+$  in a liquid scintillator. About the same time, Davis<sup>3</sup> was trying to detect the (not anti-)electron-neutrino by the radiochemical method using the reaction  $\nu_e + {}^{37}\text{Cl} \rightarrow {}^{37}\text{Ar} + e^-$ . Although this method is not suitable for the detection of  $\bar{\nu}_e$  from a nuclear reactor, this experiment motivated Pontecorvo<sup>4</sup> to discuss the possibility of  $\nu$ - $\bar{\nu}$  oscillation.

In 1964, Davis started the Homestake Experiment to observe  $\nu_e$  from the Sun by the same detection technique described above, which is good to detect (not-anti)  $\nu_e$ . Four years later, Davis<sup>5</sup> reported a deficit of the solar neutrino. This was the beginning of the “Solar Neutrino Problem”.

#### 1.2 $\nu_\mu$

The muon neutrino was “detected” in an experiment to observe Yukawa meson (i.e.  $\pi$ ) decaying into muon in 1947. In a balloon-borne emulsion experiment, Powell *et al.*<sup>6</sup> observed  $\pi^+$  decays at rest. They confirmed constant range of  $\mu^+$  indicating a two body

decay. This is also the “first observation” of the production of atmospheric neutrinos. At that time, it was not known whether they were same neutrinos as those from  $\beta$ -decay or not.

In 1962, interactions of neutrinos from the decays of  $\pi$  produced by an accelerator were observed<sup>7</sup> and confirmed that  $\nu_\mu$  is different particle from  $\nu_e$ . Soon after, Maki, Nakagawa and Sakata<sup>8</sup> discussed the possibility of  $\nu_\mu$ - $\nu_e$  oscillation when two neutrinos have different masses.

#### 1.3 $\nu_\tau$

After the  $\tau$  lepton was discovered in 1975 by Perl *et al.*<sup>9</sup>, it was thought that the  $\nu_\tau$  must exist as the third generation neutrino. However, the charged current interactions of  $\nu_\tau$  had not been observed until DONUT collaboration's report<sup>10</sup>.

### 2 Solar Neutrinos

For solar neutrino detection, there have been three types of experiments, shown in Table 1. Two of them are radiochemical experiments using chlorine or gallium. These radiochemical experiments can measure the total flux above its energy threshold. Timing information is limited by the period of chemical extraction. The other type of experiment is water Čerenkov experiment, which can measure timing and energy of each event. Kamiokande, Super-Kamiokande and SNO are this type. They can see the electron from the elastic scattering (ES)  $\nu_x + e^- \rightarrow \nu_x + e^-$ .

Table 1. Solar Neutrino Experiments

| Type                              | Experiments                                       | Process   | Energy Threshold  |
|-----------------------------------|---|---|---|
| Chlorine                          | Homestake <sup>11</sup>                           | $\nu_e + {}^{37}\text{Cl} \rightarrow {}^{37}\text{Ar} + e^-$   | $E_\nu > 817 \text{ keV}$   |
| Gallium                           | SAGE <sup>12</sup><br>Gallex+GNO <sup>13</sup>    | $\nu_e + {}^{71}\text{Ga} \rightarrow {}^{71}\text{Ge} + e^-$   | $E_\nu > 235 \text{ keV}$   |
| H <sub>2</sub> O                  | Kamiokande <sup>14</sup><br>Super-K <sup>15</sup> | $\nu_x + e^- \rightarrow \nu_x + e^-$   | $E_e > 6.5 - 7 \text{ MeV}$<br>$E_e > 5.5 \text{ MeV}$                            |
| D <sub>2</sub> O<br>(heavy water) | SNO <sup>16</sup>                                 | $\nu_x + e^- \rightarrow \nu_x + e^-$<br>$\nu_e + d \rightarrow p + p + e^-$<br>$\nu_x + d \rightarrow p + n + \nu_x$ | $E_e > 6.75 \text{ MeV}$<br>$E_e > 6.75 \text{ MeV}$<br>$E_\nu > 2.2 \text{ MeV}$ |

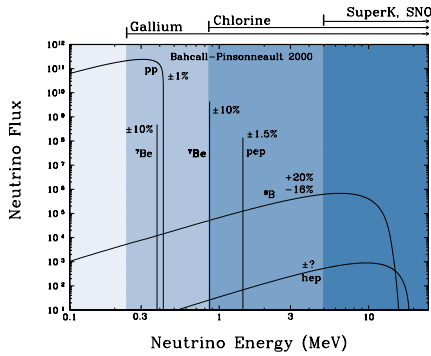


Figure 1. The SSM flux prediction as a function of energy. The sensitivity of each experiment is also shown. From <http://www.sns.ias.edu/~jnb/>

Total Rates: Standard Model vs. Experiment  
Bahcall-Pinsonneault 2000

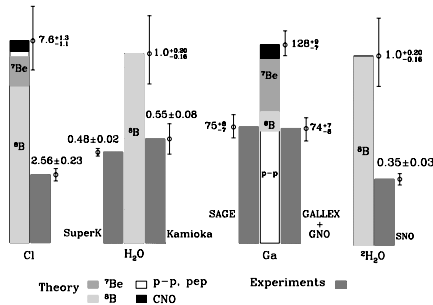


Figure 2. The SSM flux prediction with four energy thresholds corresponding to the type of experiment. From <http://www.sns.ias.edu/~jnb/>

However, SNO is a qualitatively new type of experiment, since D<sub>2</sub>O (heavy water) is used as detector media. It can also see electrons from the charged current reaction (CC)  $\nu_e + d \rightarrow p + p + e^-$ . The CC reaction is sensitive exclusively to  $\nu_e$ , while the ES reaction has a small sensitivity to  $\nu_\mu$  and  $\nu_\tau$ . The neutral current reaction (NC)  $\nu_x + d \rightarrow p + n + \nu_x$ , which is equally sensitive to all active neutrino flavors, can also be detected by  $\gamma$  from neutron capture. By measuring CC/ES flux ratio (or CC/NC flux ratio), evidence of flavor transformation can be extracted independent of solar model flux calculations.

Comparing CC flux measurement from SNO to ES flux measurement from Super-K, a  $3.3\sigma$  difference has been reported. Detailed discussions can be found elsewhere<sup>16</sup>. Assuming the oscillation hypothesis, large mixing angle solutions are favored<sup>17</sup>.

KamLAND and Borexino are experiments designed to detect low energy neutrinos using liquid scintillator. They are “real-time” detectors like water Čerenkov experiment, but the energy threshold can be lower.

KamLAND<sup>18</sup> is a long baseline reactor neutrino experiment, planning to detect  $\bar{\nu}_e$  from nuclear power reactors located  $175 \pm$

35km away. Their sensitivity for neutrino oscillations completely covers the LMA solution to the solar neutrino problem.

Borexino<sup>19</sup> is aiming to provide direct measurement of the  ${}^7\text{Be}$  neutrino flux, which is very crucial for the flux independent analysis of the solar neutrino oscillation.

### 3 Atmospheric Neutrinos

The sources of atmospheric neutrinos are charged  $\pi$ 's produced in cosmic ray reactions with nuclei of atmospheric molecules. Since  $\pi^\pm$  decays to  $\mu^\pm + \nu_\mu(\bar{\nu}_\mu)$  and  $\mu^\pm$  decays to  $e^\pm + \nu_e(\bar{\nu}_e) + \bar{\nu}_\mu(\nu_\mu)$ , the flux ratio of  $\nu_\mu/\nu_e$  is expected to be about 2. If the primary cosmic ray arrives isotropically, upward and downward symmetry is expected. But in case of neutrino oscillations, different results are expected, depending on the energy and the zenith angle (i.e. the flight length of the neutrino).

Super-K has reported their 79.3 kton-year (1289 days with 22.5kton fiducial mass) data analysis. From their  $\nu_\mu - \nu_\tau$  oscillation analysis, they got 90% C.L. allowed region at  $1.6 \times 10^{-3} \text{ eV}^2 < \Delta m^2 < 4 \times 10^{-3} \text{ eV}^2$  and  $\sin^2 2\theta > 0.89$ . Detailed discussions can be found elsewhere<sup>15</sup>.

Soudan-2 is a different type of experiment, with 963 tons of fine tracking calorimeter made of 1.5cm diameter drift tubes installed in honeycomb lattice steel cell. From preliminary results based on 5.1 kton-years data, their  $\nu_\mu - \nu_\tau$  oscillation-allowed region is consistent with Super-K.

MACRO is another type of experiment with large area streamer tubes for tracking and liquid scintillator counters for time-of-flight. From their zenith angle distribution of upward-going muons produced by atmospheric neutrinos in the rock below their detector, they observed deficit of upgoing muon flux<sup>20</sup>. It agrees well with  $\nu_\mu - \nu_\tau$  oscillations with maximal mixing around  $\Delta m^2 \sim 2.4 \times 10^{-3} \text{ eV}^2$ .

Some models predict that the atmospheric  $\nu_\mu$  deficit is due to its oscillation into "sterile" neutrinos ( $\nu_s$ ) that do not interact, even via neutral current(NC). If this is the case, the number of NC like events for upward going neutrino should also be reduced. Moreover, matter effect in the Earth suppress the oscillation at high energy region ( $E_\nu > 15\text{GeV}$ ).

Both Super-K<sup>15</sup> and MACRO<sup>20</sup> have reported that pure  $\nu_\mu - \nu_s$  oscillation is disfavored with 99% C.L.

### 4 Long Baseline Experiments (1st generation)

In order to investigate the atmospheric neutrino deficit, the K2K experiment was proposed as the first long baseline experiment using a  $\nu_\mu$  beam from an accelerator.  $3.85 \times 10^{19}$  POT were accumulated from June 1999 to April 2001. 44 events were observed while  $64_{-6.6}^{+6.1}$  events were expected. The probability of null oscillation is less than 3%. Energy spectrum analysis is underway. Detailed discussions can be found elsewhere<sup>21</sup>.

### 5 "Medium Baseline" Experiments

The LSND experiment and the KARMEN experiment use neutrinos from  $\pi^+ \rightarrow \mu^+ + \nu_\mu$  decays at rest followed by  $\mu^+ \rightarrow e^+ + \nu_e + \bar{\nu}_\mu$  decays at rest in the low energy ( $\sim 800 \text{ MeV}$ ) proton beam dump.  $\pi^-$  decay is suppressed by nuclear capture. There is a minor fraction of  $\pi^-$  decay in flight followed by  $\mu^-$  decay, which is also suppressed by capture process  $\mu^- + p \rightarrow n + \nu_\mu$ .

This gives a very small  $\bar{\nu}_e$  contamination flux below the  $10^{-3}$  level, which is further reduced by software cuts. Both experiments searched for  $\bar{\nu}_\mu \rightarrow \bar{\nu}_e$  oscillation in appearance mode by detecting the positron from  $\bar{\nu}_e + p \rightarrow n + e^+$ , and the delayed  $\gamma$  ray from neutron capture.

Figure 3 shows the  $L/E$  distribution by

Table 2. LSND and KARMEN

|                       | LSND  | KARMEN   |
|-----------------------|---|--|
| proton beam intensity | 1000 $\mu\text{A}$  | 200 $\mu\text{A}$  |
| repetition rate       | 120 Hz  | 50 Hz  |
| spill structure       | 600 $\mu\text{s}$   | 100 ns double pulse<br>(225 ns apart)  |
| baseline length       | 30 m  | 17 m   |
| detector mass         | 167 t   | 56 t   |
| liquid scintillator   | mineral oil based   | organic scintillator   |
| detector structure    | 5.7m $\phi$ $\times$ 8.3m cylinder<br>(water Čerenkov like) | 512 segmented rectangular modules<br>with $Gd_2O_3$ coated paper<br>within the acrylic module wall |
| neutron detection     | $n + p \rightarrow d + \gamma$ (2.2MeV)                     | $n + Gd \rightarrow Gd + \gamma$ (8MeV)  |

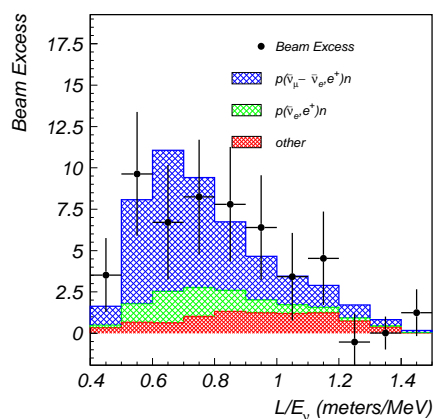


Figure 3. The  $L_\nu/E_\nu$  distribution for events observed by LSND. The expected distribution from backgrounds and  $\bar{\nu}_\mu \rightarrow \bar{\nu}_e$  oscillations at low  $\Delta m^2$  are also shown. From *Phys. Rev. D* **64**, 112007.

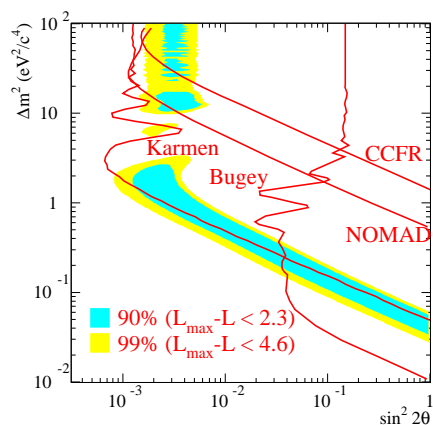


Figure 4. The allowed region of neutrino oscillation parameter by the LSND experiment is shown shaded. Also shown are the excluded regions (90% C.L.) by the KARMEN, NOMAD, CCFR and Bugey experiment. From *Phys. Rev. D* **64**, 112007.

LSND. The LSND result gives evidence for an excess of  $\bar{\nu}_e$  events, while KARMEN result<sup>23</sup> does not support it. Comparison of both experiments is shown in Table 2.

Figure 4 shows the allowed region of oscillation parameters describing LSND result, with excluded regions by other experiments. A narrow region still remains as a possible region for  $\bar{\nu}_\mu \rightarrow \bar{\nu}_e$  oscillation.

The primary goal of the Mini-BooNE<sup>24</sup> experiment is to confirm or disprove the neutrino oscillation signal suggested by LSND. The neutrino beam is produced by 8GeV protons from the Fermilab Booster with horn focusing and variable (25 to 50m) decay path. The detector is a 769 ton (445 ton fiducial) pure mineral oil Čerenkov detector installed 500m away from the production target. A  $\nu_\mu \rightarrow \nu_e$  oscillation to explain LSND results would produce 1000  $\nu_e$  charged current (CC) events, while 500,000  $\nu_\mu$  CC events and 1700  $\nu_e$  CC events due to the intrinsic  $\nu_e$  component are expected.

## 6 Short Baseline Experiments

The CHORUS and NOMAD experiments searched for  $\nu_\mu \rightarrow \nu_\tau$  oscillation in the  $\Delta m^2 > 1\text{eV}^2$  region, which corresponds to the  $\nu_\tau$  mass as the hot component of the Dark Matter of the Universe. They were installed one behind the other in the wide-band neutrino beam from the CERN 450 GeV proton synchrotron. The average neutrino energy was about 27 GeV and the distance between the neutrino source and detector was  $\sim 600\text{m}$  on average. The intrinsic  $\nu_\tau$  component in  $\nu_\mu$  beam was as low as  $3.3 \times 10^{-6}$   $\nu_\tau$  charged current (CC) interaction per  $\nu_\mu$  CC interaction. The  $\nu_\tau$  is identified by detecting  $\tau^-$  produced by  $\nu_\tau$  CC interaction. CHORUS and NOMAD employ two different approaches to identify  $\tau^-$  decay.

NOMAD uses a purely kinematical tech-

nique to identify  $\nu_\tau$  CC interaction. Precise measurements of the secondary particle momenta are required. The core of the detector consisted of 2.7 tons of fiducial mass made of a series of drift chambers in a 0.4 Tesla magnetic field, acting both as target and as spectrometer. The  $\nu_\tau$  CC interaction is differentiated essentially by selecting events using three vectors: the missing transverse momentum, the transverse momentum of hadron jet, and the transverse momentum of the  $\tau$  decay track(s). Figure 5 shows the final NOMAD results<sup>25</sup> on  $\nu_\mu - \nu_\tau$  and  $\nu_e - \nu_\tau$  oscillations together with the results by other experiments. The two flavor mixing limit is excluded down to  $\sin^2 2\theta_{\mu\tau} < 3.3 \times 10^{-4}$  at large  $\Delta m^2$  and  $\sin^2 2\theta_{e\tau} < 1.5 \times 10^{-2}$  at large  $\Delta m^2$ .

CHORUS used nuclear emulsion acting as the target and as detector of the interaction vertex and the decay of  $\tau^-$  lepton. The nuclear emulsion can provide a three dimensional topology of charged tracks with sub- $\mu\text{m}$  spatial resolution. 0.77 tons of nuclear emulsion was exposed to the neutrino beam with an integrated intensity corresponding to  $5.06 \times 10^{19}$  proton on target. The search for  $\nu_\tau$  interaction has been performed for the muonic (“ $1\mu$ ”) and the hadronic (“ $0\mu$ ”) one prong decay.

In Phase-I analysis,  $\sim 1.7 \times 10^5$  neutrino interactions have been located in the emulsion and no  $\tau$  candidate event was observed, while 0.1 and 1.1 background events were expected for  $1\mu$  and  $0\mu$  samples respectively. The 90% C.L. excluded region from CHORUS Phase-I result<sup>26</sup> is also shown in Figure 5. The mixing limit is excluded down to  $\sin^2 2\theta_{\mu\tau} < 6.8 \times 10^{-4}$  at large  $\Delta m^2$ . This number can not be directly compared to NOMAD result, since the statistical treatment<sup>27</sup> of the data is different. Using the same statistical treatment<sup>28</sup> as the NOMAD experiment for comparison,  $\sin^2 2\theta_{\mu\tau} < 4.4 \times 10^{-4}$  at large  $\Delta m^2$  is obtained.

To improve sensitivity, CHORUS contin-

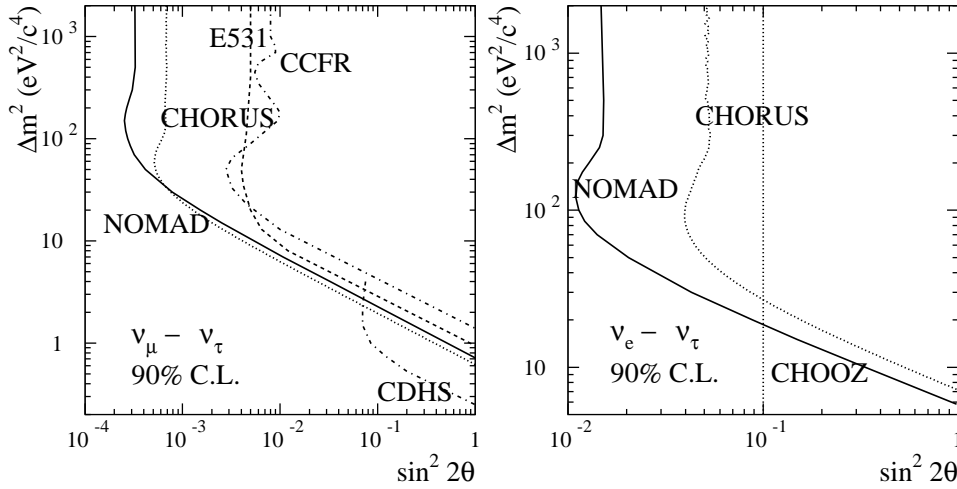


Figure 5. Contours outlining a 90% C.L. region in the  $\Delta m^2$  -  $\sin^2 2\theta$  plane for  $\nu_\mu - \nu_\tau$  oscillation (left) and  $\nu_e - \nu_\tau$  oscillation (right). From *Nucl. Phys. B* **611**, 3 (2001).

ues Phase-II analysis with a new scanning method, called “Netscan”, developed in the DONUT experiment described below. Improvement is expected by higher kink finding efficiency and electron identification to search electronic decay mode of the  $\tau$ . As an example of the power of “Netscan” method in Phase-II analysis, from  $\sim 2.5 \times 10^4$   $\nu_\mu$  CC interactions, 283  $D^0$  meson decay is observed with an estimated background of 9.2  $K^0$  and  $\Lambda$  decays<sup>29</sup>.

The DONUT experiment has observed the charged current interactions of  $\nu_\tau$  by identifying the  $\tau$  lepton as the only lepton created at the interaction vertex.

The neutrino beam was created using 800 GeV protons from the Fermilab Tevatron interacting in a one meter long tungsten beam dump. The nuclear emulsion target was placed 36m downstream from the dump.  $\nu_e$ ,  $\nu_\mu$  and  $\nu_\tau$  that interacted in the emulsion target mostly originated from the decays of charmed mesons in the beam dump. But  $\nu_\mu$  also had large (about half) component from  $\pi$  and  $K$  decays. The primary source of  $\nu_\tau$  is the leptonic decay of a  $D_S^\pm$  meson into  $\tau^\pm + \nu_\tau(\bar{\nu}_\tau)$ , and the subsequent decay of the

$\tau^\pm$  to  $\bar{\nu}_\tau(\nu_\tau)$  + anything. The other products from the beam dump, mostly muons, were absorbed or swept away from the emulsion region using magnets with concrete, iron and lead shielding. The length of exposure for each target was set by the accumulated track density of muon, with a limit of  $10^5$   $\text{cm}^{-2}$  for the analysis.

ECC (“Emulsion Cloud Chamber”) module had a repeated structure of emulsion plates interleaved with 1 mm thick stainless steel sheets. Scintillating fiber trackers, distributed between the emulsion modules, were used to reconstruct vertex and provide the information to locate vertex in the emulsion module. The spectrometer downstream provided the information about lepton identification and energy measurement.

A total of  $4.0 \times 10^6$  triggers were recorded from  $3.54 \times 10^{17}$  protons incident on the tungsten beam dump. From the spectrometer information, 898 events were selected as neutrino interaction candidates, and 727 of them had a predicted vertex within a fiducial emulsion volume. Among them, 566 events were scanned to locate a vertex using “Netscan” method<sup>30</sup> as follows.

All track segments in entire predicted

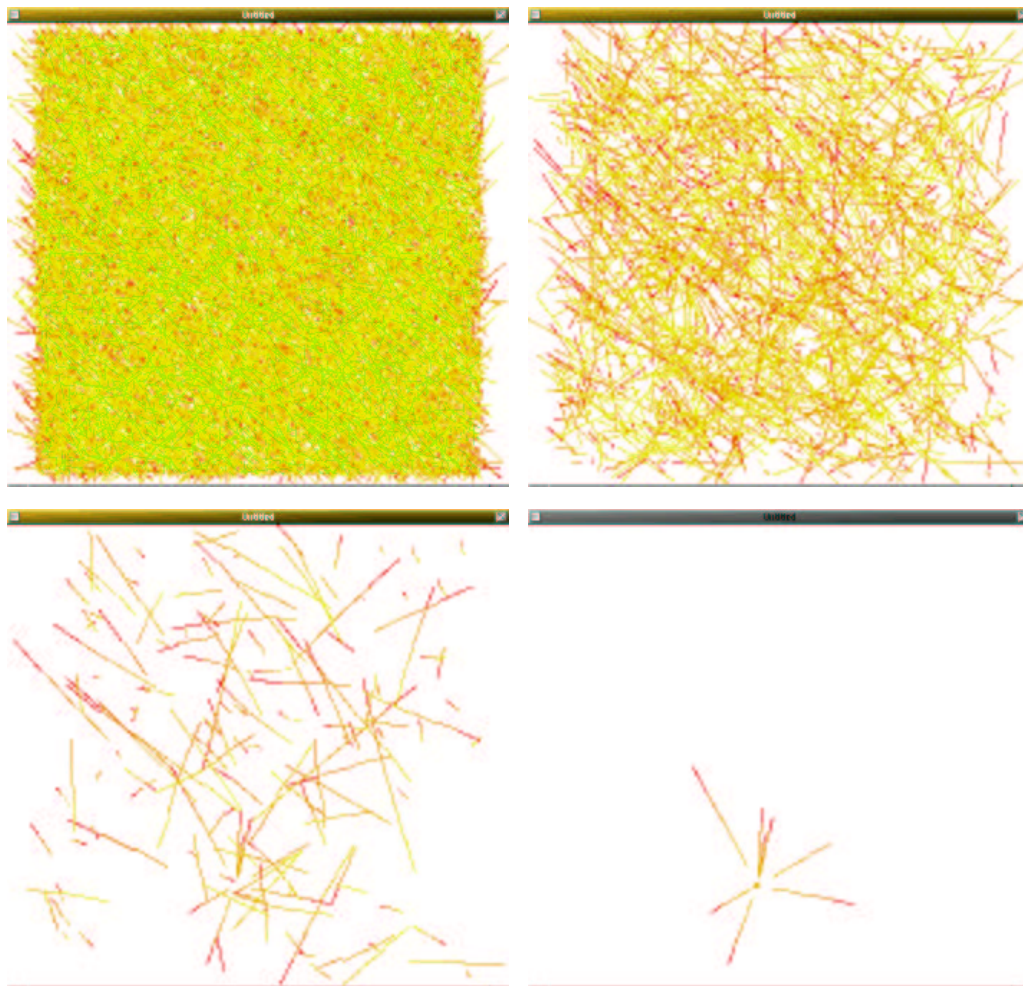


Figure 6. Example of NETSCAN in the DONUT experiment.

- (top left) after alignment
- (top right) after rejection of penetrating track
- (bottom left) after rejection of non-connected track
- (bottom right) after requiring a small impact parameter

Table 3.  $\tau$  candidate in DONUT

|                     | $\tau$ | charm<br>BG | hadronic<br>int. BG |
|---------------------|--------|-------------|---------------------|
| short flight        | 1      | 0.13        | 0.22                |
| long flight<br>kink | 4      | 0.30        | 0.27                |
| trident             | 2      | 0.61        | 0.08                |
| total               | 7      | 1.04        | 0.57                |

volume are read out by the fully automated system, called the Ultra Track Selector<sup>31</sup>. A typical scanning volume is  $5\text{mm} \times 5\text{mm}$  in the transverse direction and  $\sim 15\text{mm}$  in the longitudinal direction, typically corresponding to 12 emulsion plates. There are approximately  $10^4$  track segments found in each emulsion plate. Tracks that are recognized as passing through the volume are used for plate-to-plate alignment and are eliminated as candidate tracks from a neutrino interaction. The distance of closest approach between any two tracks that started in the same or neighboring emulsion plate is calculated and those within  $4\ \mu\text{m}$  are retained as candidates to form a two-track vertex. From the cluster of two-track vertices, the interaction vertex is identified. An example is shown in Figure 6

Out of 566 events, a valid vertex was located for 344 events. To 337 out of the 344 events, systematical decay search was applied and 7  $\tau$  candidates were identified as shown in Table 3. The main sources of backgrounds are the decays of charmed particles produced by  $\nu_\mu$  or  $\nu_e$  CC interaction with inefficient lepton identification at the interaction vertex, and hadronic interactions in the steel plate. The total background is estimated to be 1.61 events (preliminary result).

## 7 Long Baseline Experiments (2nd generation)

In addition to KamLAND, there are three long baseline projects shown in Table 4. They are planning to perform high precision measurements of spectrum distortion in  $\nu_\mu$ -disappearance, high precision measurements of mixing angle, or  $\nu_\tau$ -appearance detection in order to establish the clear evidence of oscillation at  $\Delta m^2$  region by atmospheric neutrino experiments.

The MINOS<sup>32</sup> detector consists of 2.54 cm thick magnetized iron interleaved with 4cm wide, 1 cm thick and 8 m long scintillator strips with wavelength shifting fiber read-out, which provides both calorimetric and tracking information. NC/CC ratio can discriminate  $\nu_\mu \rightarrow \nu_\tau$  and  $\nu_\mu \rightarrow \nu_s$ .

The JHF-Kamioka neutrino project<sup>33</sup> plans the high precision measurement of neutrino mass and mixing. The first phase using the Super-Kamiokande detector plans

- (1) an order of magnitude better precision in the  $\nu_\mu \rightarrow \nu_\tau$  oscillation measurement.
- (2) a factor of 20 more sensitive search in the  $\nu_\mu \rightarrow \nu_e$  appearance.
- (3) a confirmation of the  $\nu_\mu \rightarrow \nu_\tau$  oscillation or discovery of  $\nu_s$  by detecting the neutral current events.

Both ICARUS and OPERA are  $\nu_\tau$  appearance search experiments.

The ICARUS<sup>34</sup> detector is a liquid Argon time projection chamber with  $\sim 1$  mm spatial resolution in three dimensional reconstruction capabilities. For  $\tau^-$  identification, the kinematical approach is used like NOMAD.

The OPERA<sup>35</sup> experiment uses same detection technique as the DONUT experiment. The building unit of the detector is an ECC ("Emulsion Cloud Chamber") brick, consisting of machine-coated emulsion films interleaved with 1mm thick lead plates. 0.23 mil-

Table 4. Future Long Baseline Project

|                             | NuMI                       | JHF-Kamioka              | CNGS                       |
|-----------------------------|----------------------------|--------------------------|----------------------------|
| accelerator                 | Main Injector (Fermilab)   | JHF (JAERI)              | SPS (CERN)                 |
| experiment                  | MINOS                      | Super-K                  | ICARUS/OPERA               |
| proton beam energy          | 120 GeV                    | 50 GeV                   | 400 GeV                    |
| proton beam intensity       | $4.0 \times 10^{13}$ ppp   | $3.3 \times 10^{14}$ ppp | $4.8 \times 10^{13}$ ppp   |
| machine cycle               | 2.0 sec                    | 3.4 sec                  | 6 – 27 sec                 |
| proton on target            | $3.7 \times 10^{20}$ /year | $1 \times 10^{21}$ /year | $4.5 \times 10^{19}$ /year |
| baseline length             | 732 km                     | 295 km                   | 730 km                     |
| mean $\nu$ energy           | 6.8(5.2,12) GeV            | 0.7 GeV                  | 17 GeV                     |
| number of $\nu_\mu$ CC int. | 1270(470,2740)/kt/year     | 100/kt/year              | 3200/kt/year               |
| fiducial mass               | 3.3 kt                     | 22.5 kt                  | 1.2 kt / 1.8 kt            |

lions of bricks will be used to build a 1.8 kton target. Using information from an electronic detector, the bricks containing the neutrino interaction will be extracted on a daily basis. The emulsion analysis will progress simultaneously with the exposure. For  $\Delta m^2 = 2.5 \times 10^{-3} \text{eV}^2$ , 2.8  $\tau$  event/year is expected while 0.11 background event/year is expected.

## 8 Summary

SNO has begun a new era of measurements of Solar neutrinos, and the large mixing angle solutions seem to be favored. KamLAND has good chance to get a positive result.  ${}^7\text{Be}$  neutrino detection by Borexino is also crucial.

LSND's large  $\Delta m^2$  solutions are excluded. But its small  $\Delta m^2$  solutions are still possible, which will be covered by Mini-BooNE.

From the atmospheric neutrino experiments,  $\nu_\mu \rightarrow \nu_\tau$  is favored over  $\nu_\mu \rightarrow \nu_s$ . And DONUT confirmed that  $\nu_\tau$  does interact in the same manner as  $\nu_e$  and  $\nu_\mu$ . The next step is getting clear evidence of oscil-

lations by  $\nu_\tau$  appearance detection and high precision measurements of the oscillation parameter.

## Acknowledgments

I thank Byron Lundberg, Naoki Nonaka and Masahiro Komatsu for their help for this article. I am also grateful to Juliet Lee Franzini for her encouragement to complete this article.

## References

1. J. Chadwick, *Verhandl. Dtsch. phys. Ges.* **16**, 383 (1914).
2. C.L. Cowan et al., *Science* **124**, 103 (1956).
3. R. Davis Jr., *Phys. Rev.* **97**, 766 (1955).
4. B. Pontecorvo, *JETP(USSR)* **34**, 247 (1958).
5. R. Davis Jr. et al., *Phys. Rev. Lett.* **20**, 1205 (1968).
6. G.P.S. Occhialini and C.F. Powell, *Nature* **159**, 186 (1947).
7. G.T. Danby et al., *Phys. Rev. Lett.* **9**,

- 36 (1962).
8. Z. Maki, M. Nakagawa and S. Sakata, *Prog. Theo. Physics* **28**, 247 (1962).
  9. M.L. Perl et al., *Phys. Rev. Lett.* **35**, 1489 (1975).
  10. M. Nakamura, *Nucl. Phys. B* (Proc. Suppl.) **77**, 259 (1999).  
K. Kodama et al., *Phys. Lett. B* **504**, 218 (2001).
  11. B.T. Cleveland et al, *Astrophys. J. B* **496**, 505 (1998).
  12. J.N. Abdurashitov et al, *Phys. Rev. C* **60**, 055801 (1999).  
V. Gavrin et al, *Nucl. Phys. B* (Proc. Suppl) **91**, 36 (2001).
  13. M. Altman et al, *Phys. Lett. B* **490**, 16 (2000).  
E. Bellotti et al, *Nucl. Phys. B* (Proc. Suppl) **91**, 44 (2001).
  14. Y. Fukuda et al, *Phys. Rev. Lett.* **77**, 1683 (1996).
  15. J. Goodman, these proceedings.  
S. Fukuda et al, *Phys. Rev. Lett.* **86**, 5651 (2001).  
S. Fukuda et al, *Phys. Rev. Lett.* **85**, 3999 (2000).
  16. J. Klein, these proceedings.  
Q.R. Ahmad et al., *Phys. Rev. Lett.* **87**, 071301 (2001).
  17. Fogli, Lisi, Montanino and Palazzo, *Phys. Rev. D* **64**, 093007 (2001).  
Bahcall, Gonzalez-Garcia and Pena-Garay, *JHEP* **0108**, 014 (2001).
  18. A. Piepke et al, *Nucl. Phys. B* (Proc. Suppl) **91**, 99 (2001).
  19. G. Alimonti et al, *Astropart. Phys.* **16**, 205 (2002).
  20. M. Ambrosio et al., *Phys. Lett. B* **517**, 59 (2001).
  21. C.K. Jung, these proceedings.
  22. A. Aquilar et al., *Phys. Rev. D* **64**, 112007 (2001).
  23. K. Eitel et al, *Nucl. Phys. B* (Proc. Suppl) **91**, 191 (2001).
  24. A.O. Bazarko et al, *Nucl. Phys. B* (Proc. Suppl) **91**, 210 (2001).
  25. P. Astier et al., *Nucl. Phys. B* **611**, 3 (2001).
  26. E. Eskut et al., *Phys. Lett. B* **497**, 8 (2001).
  27. T. Junk, *Nucl. Instr. and Meth. A* **434**, 435 (1999).
  28. G.J. Feldman and R.D. Cousins, *Phys. Rev. D* **57**, 3873 (1998).
  29. A. Kayis-Topaksu et al., *CERN-EP* 2002-005 (2002).  
to be published in *Phys. Lett. B*.
  30. K. Kodama et al., to be published in *Nucl. Instr. and Meth.*
  31. S. Aoki et al., *Nucl. Instr. and Meth. B* **51** 466 (1990).  
T. Nakano, *Ph.D Thesis, Nagoya Univ.*, (1997).
  32. S.G. Wojcicki, *Nucl. Phys. B* (Proc. Suppl) **91**, 216 (2001).
  33. Y. Itow et al., [hep-ex/0106019] (2001)
  34. A. Rubbia, *Nucl. Phys. B* (Proc. Suppl) **91**, 223 (2001).  
F. Arneodo et al., [hep-ex/0103008] (2001))
  35. M. Gular et al., *CERN/SPSC 2000-028*, *SPSC/P318, LNGS P25/2000*, (2000).